

# UA9 report for 2013

## Executive Summary

This report describes the progress of UA9 of the last 12 months from October 2012. Since no beams were available for the SPS UA9 runs during the 2013 operation with ions, most of the efforts of the UA9 Collaboration were devoted to preparing the prototype crystal collimation system for LHC and to improving the UA9 equipment installed in the SPS. The installation in IR7 of test devices for crystal-assisted collimation in LHC is being prepared. The layout has been chosen to reduce significantly the local losses at the limiting locations of the present collimation system, taking into account the optical constraints of the collimation insertion. A goniometer suitable for orienting and positioning the crystal with an angular accuracy of the order of 1  $\mu$ rad required for the LHC operation was designed in collaboration with industrial partners. The adopted solution is based on a mechanical linear stage and a piezoelectric rotational stage that guarantee a linear variation of the angular orientation of the crystal also during the dynamical transients of angular adjustments. At the end of 2012, a preliminary test in the HiRadMat facility at CERN was performed consisting in the repeated irradiation of a crystal with several nominal bunches of protons at the LHC injection energy. No damage was detected by visual inspection, whilst the crystal will undergo after radiation cool-down a test to evaluate its deflection efficiency. The design of a detector based on Cherenkov radiation suited to detect the halo particles deflected by a crystal in the vacuum pipe of the SPS and LHC is almost completed. Preliminary tests were performed at the BTF facility of the INFN-LNF in Frascati, to optimize the shape of the quartz radiator. Plans have been formulated to improve the functionality of the UA9 devices in the SPS that will be possibly implemented before the SPS start-up in 2014. A new version of the horizontal-vertical roman-pot having a reduced impact on the local primary vacuum and on the impedance budget will be built. A prototype version of the in-vacuum Cherenkov detector will be installed in the SPS vacuum pipe to gain experience in view of using it in LHC. Multi-strip crystal for deflecting halo particles by multi-reflection will be tested and compared to single crystals operated in channeling mode.

Several publications were issued to illustrate the UA9 results. The simulation challenges and methods used to interpret the SPS experimental data were reported in NIM B 313 (2013) 26-32. Issues for crystal deflectors for high-energy ion beams were described in Nuclear Physics News, Vol.23, No. 3, 2013 p 46-49. Data on dechanneling length for high-energy pions, collected in 2010 and yet unpublished, were reported in Phys. Lett. B 719 (2013) 70-



73. A review of UA9 results and of the future UA9 strategy was included in the EuCARD-Rep-2013-002, in the frame of the FP7 Research Infrastructure project EuCARD, funded by the EU, grant agreement no. 227579. The HiRadMat data were reported at the IPAC13 accelerator conference. Reviews of the UA9 results were also presented at the Conference of the Italian Physical Society in Trieste, at the 13<sup>th</sup> topical Seminar on Innovative Particle Detectors (IPRD13) in Siena and the AFTER@LHC meeting in Trento.

One trainee joined UA9 in 2013. Two PhD theses are in progress.

### **Recall of the main UA9 findings in 2012**

The results described below are extracted from Ref [1, 2].

The UA9 results, collected in 2012 in the SPS with protons and Pb ions at 120 GeV/c and 270 GeV/c per charge, gave additional evidence of our understanding and our ability to master crystal-assisted collimation.

1. With a 1 mm-long crystal, fully suited to the SPS stored beam energy, in channeling orientation the loss rate recorded downstream the crystal is reduced by a factor of about 20 whilst the loss rate in the dispersion suppressor downstream of the crystal is reduced by a factor 7.
2. The angle between the crystal planes and crystal surface exposed to the beam halo is called crystal miscut angle. Its value plays an important role in the halo deflection process. When taking it into account, the UA9 experimental data become in an excellent agreement with simulation results.
3. The beneficial effect of using a crystal primary collimator to deflect the beam halo is global. Although the electronics of the SPS beam loss monitors is not fully adequate for the UA9 running conditions, consistent and reliable indications are available on the fact that the loss map around the entire SPS circumference shows strong reduction of losses in channeling orientation.
4. The first mechanical goniometer compliant with the LHC specification was made available in collaboration with industrial partners.

### **Optimization of the gap between the crystal and the absorber in the SPS**

The possibility for optimization of crystal-assisted collimation has been studied at the SPS with stored beams of protons and Pb ions with 270 GeV/c per unit charge. The data were

collected in 2012 and analyzed in 2013. It was shown that the collimation leakage is minimal for some values of the absorber offset relative to the crystal. The optimal offset value is larger for Pb ions because of their considerably larger ionization losses in the crystal, which cause large increases of particle betatron oscillation amplitudes. The optimal absorber offset allows obtaining maximal efficiency of crystal-assisted collimation. Detailed results are presented in Ref. [3].

### **Cristal-assisted collimation in LHC**

Following the past recommendations of the SPSC referees, the conclusions of the 107th LHCC meeting and the quality of the experimental results recently collected in the SPS, the UA9 Collaboration focused the recent activities on the extension of the experiment to the LHC, with the aim to prove the crystal-aided halo suppression at the LHC. The main goal is to allow a direct comparison of the collimation cleaning efficiency with and without the use of crystals. The test in LHC is called hereafter the LUA9 experiment. The proposal for the installation in the LHC has been brought forward (LHC Engineering Change Request to define the scope of LS1 works is under approval).

A layout for LUA9 has been worked out that introduces the minimum number of extra devices in the standard LHC layout, making profit of the already existing beam instrumentation and of the collimators in place. The experiment will be installed only on Beam 1 of the LHC, the one that runs clockwise, and will be inserted in the betatron collimation region in Interaction Region 7 (IR7). Tests will be performed during dedicated machine development periods at low intensity, at both injection and collision energy. The experiment will be carried out both in the horizontal and in the vertical plane of betatronic oscillations. For each plane a goniometer capable to position the crystal with high precision and an in-vacuum Cherenkov detector have been planned. A staged installation has been foreseen, with the two goniometers, one horizontal and one vertical, being installed before the end of Long Shutdown 1, together with all the cabling and the infrastructure necessary also for the detectors. The installation of the detectors will be requested at a later time, during the first useful technical stop or winter shutdown after the next LHC startup.

Care has been taken that the additional devices would be masked, and therefore invisible to the beam, during ordinary LHC operation, in order to keep unchanged the impedance budget and to avoid the onset of coherent instabilities at high circulating intensity.

Cleaning considerations guided the selection of the horizontal and vertical crystal /goniometer positions. Unpublished results of tracking simulations, indeed, predict a cleaning efficiency 5 to 10 times better than with the present collimation system.

A schematic layout of the collimation system in IR7 with the positions of the devices of the LUA9 experiment is shown in Fig. 1. The LUA9 absorbers are part of the standard collimation system already in place in LHC. The Cherenkov detectors will be installed a short way upstream the corresponding absorber in order to detect the deflected beam before it impinges onto the absorber. Fig. 2 and Fig. 3 show the trajectories of the channeled particles in the horizontal plane with respect to the  $6\sigma$  circulating beam at injection and at collision energy. Similar layouts were designed for the vertical halo case. After being deflected by the crystal, halo particles are intercepted by existing secondary collimators that will be used as absorbers. Cherenkov detectors might be added for diagnostics purposes upstream of the absorbers.

LUA9 should allow testing crystal-assisted collimation in both the horizontal and the vertical planes of beam 1 at all the operating energies in 2015 and/or 2016.

### **High-precision goniometer**

High-precision goniometers positioned with stepping-motors have been thoroughly investigated. Their specifications are fully compliant with the requirements of the LUA9 experiment in LHC, although they should be used also in the SPS. Initially, three designs have been proposed and tested. In all of them the rotational movement is achieved by transforming a linear movement with a lever arm. In all of them, a particular attention is paid to the linearity of the transformation and to the accuracy of the rotational movement. Care is also taken to minimise the mechanical play and coupling between the linear and angular movement.

In order to satisfy the specifications on control robustness and reliability within the harsh environmental conditions, the linear axes are actuated by hybrid stepping motors and the positioning is therefore performed in open loop, which represents a more robust control solution. Linear Variable Differential Transformers (LVDT) are chosen to monitor the linear positioning of the axes, to guarantee reliability in harsh conditions and to improve the positioning accuracy and the control robustness. The results of the deep metrological characterization on the prototype realized have shown mainly the fulfillment of all the specifications in steady conditions. On the other hand, an overshoot of the linear and angular

positioning has been observed and partly mitigated. The residual uncertainty of the goniometer orientation due to the overshoot in dynamic mode may reduce the possibility of changing the crystal orientation with a sufficient precision, e.g. during the energy ramp.

To overcome the angular accuracy issue, the piezoelectric actuated goniometer, shown in Fig. 4, has been proposed that can guarantee the following functionality:

- i. Move the crystal linearly and perpendicular to the beam with a stroke of 60 mm and a linear resolution of 5  $\mu\text{m}$ .
- ii. Rotate the crystal through a total yaw angular range of  $\pm 10$  mrad with an angular resolution of 0.1  $\mu\text{rad}$  and angular accuracy of  $\pm 1$   $\mu\text{rad}$  over a linear stroke of 10 mm from the beam axis.
- iii. Perform steps in the yaw angle with an overshoot of  $< 10\%$  and a settling time to within 99% of the final value of 20 ms.
- iv. Function correctly after a bake out at a temperature of 110  $^{\circ}\text{C}$ .
- v. Function correctly up to a total accumulated radiation dose of 10 MGy.
- vi. Be easily installed using the LHC Collimator quick plug support system.
- vii. Be transparent to normal LHC operation.

The design incorporates a piezoelectric actuated rotational stage mounted on a high precision linear axis, which together allow the rotational and linear specifications to be satisfied. Piezoelectric actuators have been independently tested at the premises of the industrial partners and at CERN, to ensure the required functionality and performance. The mechanical parts for the linear displacement of the crystal are identical or very similar to those of the previous mechanical goniometers, which have already been demonstrated to fulfill our requirements. Furthermore the piezoelectric goniometer includes a second linear axis that moves, perpendicularly to the first linear axis, a section of beam pipe in and out of a position that is axially aligned with the LHC beam pipe. The piezoelectric goniometer has two working modes: the beam and the parking modes, respectively. The “beam mode”, shown in Fig. 5, is used during Machine Development, when the beam pipe section is removed and the crystal can be moved towards the beam and oriented for halo particle deflection. The “parking mode”, shown in Fig. 6, is used during normal LHC operation, when the crystal is withdrawn to a parking position and the beam pipe section is moved into a position that is axially aligned with the neighbouring, fixed beam pipe. In the parking mode the goniometer is completely transparent to normal operation and its impedance is negligible.

The high accuracy of the rotational positioning is achieved using real-time, closed-loop control of the crystal rotational position having an interferometric system as the feedback sensor. The parasitic angles in the planes perpendicular to the operational one are corrected

during crystal installation by fine-tuning adjustment stages. The high precision linear stage is actuated by a hybrid stepping motor and its guidance system is designed for high repeatability and decoupling of the linear position from the angular position.

The piezoelectric goniometers for horizontal and the vertical planes are identical and should be installed rotated by 90° degrees. A pair of them is under construction at the premises of an industrial partner and will to be delivered at CERN by the end of 2013. After a deep metrological test that should confirm the design specifications, the goniometers equipped with appropriate single crystal should be installed in IR7.

### **Crystal irradiation test**

Crystal deflectors for crystal-assisted collimation could accidentally be exposed to a not negligible fraction of the nominal beam intensity. In these extreme conditions, a reliable knowledge of thermal and radiation effects is required, to prevent the potential degradation of the channeling efficiency and, in the worst case, the mechanical stability. In particular, one concern to be addressed is the crystal integrity in case of an accidental scenario such as an asynchronous beam dump or a badly steered injection of a particle batch where bunches could be deflected onto the crystal. A first indication of possible effects on crystal deflectors can be inferred from previous irradiation tests with high-energy proton beams performed at different facilities [4, 5], where no macroscopic damage but some degradation of the channeling efficiency was observed for an irradiation density of  $2.4 \times 10^{20}$  protons/cm<sup>2</sup> at 440 GeV. However, to realistically probe the mechanical strength of a crystal under beam impact conditions imposed by the LHC operational environment, dedicated irradiation tests have been carried out at the CERN HiRadMat facility. The test in Ref [6] was performed with a 440GeV proton beam irradiating a 3 mm-thick silicon strip crystal produced at INFN-Ferrara, with properties comparable to those of the LHC deflecting crystals. The tests were carried out with the crystal in amorphous orientation. The experimental setup was accommodated in an aluminum tank equipped with glass windows permitting a visual inspection of the interior equipment (see Fig. 7). Tube extremities with 250 μm-thick beam windows made of beryllium were installed at the up- and downstream face of the tank, ensuring the containment of projected material debris in case of a potential crystal break-up. The crystal, mounted vertically on an aluminum holder, was deliberately rotated by 1° about its vertical axis to rule out channeling or volume reflection.

The crystal was aligned to the incoming beam position and high-intensity pulses were extracted from the SPS. The normalized transverse emittance as measured with the SPS beam

wire scanner before the high-intensity extractions was approximately 3.5  $\mu\text{mrad}$  in both planes, confirming the desired beam size at  $1\sigma$  of  $0.5\times 0.5\text{ mm}^2$  at the position of the crystal. Starting initially with a single bunch, the number of bunches per pulse was gradually increased to 72, 144 and 288 with an average bunch intensity of  $1.1\times 10^{11}$ . The integrated number of protons extracted during all high-intensity shots was approximately  $2\times 10^{14}$ .

First visual inspections indicate no macroscopic damage to the crystal. A key point is however the accuracy of the adopted beam-based alignment procedure, which is estimated to be 0.5 mm. With such a misalignment, the fraction of protons hitting the crystal should be decreased to less than 50% of the incident protons. Activation measurements, performed after the tests suggest that this is a plausible estimate of the fraction of the incoming beam incident on the crystal. Further post-irradiation studies of crystal properties are foreseen after a period of radiation cool-down.

### **In-vacuum Cherenkov detector**

In UA9 there are three Cherenkov radiators installed in the primary vacuum of the SPS beam pipe. The first is located close to the crystal stations, the second close to the secondary absorber and the third in the dispersion suppressor area. In 2012, a thinner radiator, shown in Fig 8, was installed in the second position, in view of optimizing the intensity of the emitted light. However the observed Cherenkov signals, although well correlated with the beam loss rate, were inappropriate to provide the precise counting of the impinging particles. Indeed, simulations have shown that a much better signal should be recorded if the radiator is inclined by  $45^\circ$  with respect to the incoming particles and the light is extracted through quartz fibers.

A rudimentary setup was assembled to check the simulation results at the BTF facility of the INFN-LNF in Frascati. A quartz radiator  $10.1\times 20.1\times 105\text{ mm}^3$  was coupled to a photomultiplier through 25 quartz fibers 120 mm long with an optical coupling efficiency estimate to 10 %. The setup was exposed to the 500 MeV  $e^-$  beam of the BTF in July 2013, giving the immediate evidence of a strong dependence of the signal on the angle of the incoming particles with the quartz radiator finger. In Fig. 9 some of the collected data are shown. The signal of the photomultiplier is plotted as a function of the incoming electrons, both for an angle of  $0^\circ$  and  $45^\circ$ . In the latter case the signal is considerably larger for all the recorded intensities, even if some sign of saturation is visible.

A so-called “hokey stick” configuration of the radiator is envisaged for a better integration of the inclined radiator in the SPS or in the LHC, as shown in Fig. 10. In our plans, a similar radiator will be tested soon at the BTF and at a later stage in the SPS.

### **Perspective and Plans**

The perspective of the Collaboration includes some ambitious milestones.

In the SPS, the goal is to install a multi-strip crystal and to compare its behavior to that of a single strip crystal. Another goal is to install a “hokey stick” shaped Cherenkov radiator and to test it in view of a possible usage in LHC.

In the H8 area, the plan is to test ultrathin single crystal, with the aim of checking if they can produce parallel beams in channeling orientation. Another goal is to test multistrip crystal with an optimal mutual orientation of the strips for a further test of multi-reflection in the SPS. Test of crystals for LHC are also envisaged. Finally, studies of possibility to increase the channeling efficiency using the crystals with decreasing curvature and the crystals with focusing slot will be pursued.

In LHC, our priority is to install in IR7 a minimal setup that includes a horizontal and a vertical piezoelectric goniometer with the associated crystal. This setup is expected to have no detrimental effect on the high-intensity high-energy operation, whilst it should allow dedicated verifications at low intensity of the beneficial effects on the collimation efficiency.

In view of these plans, the Collaboration would like to request in 2014 10 days in H8 with proton microbeams at 450 GeV and 2 dedicated days in the SPS to test the high accuracy goniometer, the new quartz detector and the multistrip crystal.

### **References**

- [1] UA9 status report for 2012.
- [2] W. Scandale et al., Phys.Letters B 714 (2012) 231.
- [3] W. Scandale et al. Optimization of the crystal assisted collimation of the SPS beam. Phys. Lett. B 726 (2013) 182.
- [4] C. Biino et al., Proceedings of EPAC96, Sitges, Barcelona, Spain, 1996, p. 2385.
- [5] V.M. Biryukov et al., Nucl. Inst. Meth. B 234, 2005, p. 23.



[6] A. Lechner et al, Proceedings of IPAC 2013, Shanghai, China, 2013, p. 3427.

### **Figure captions**

FIG. 1. Minimal layout of the LUA9 experiment in the LHC.

FIG. 2. Simulation of the horizontal crystal-assisted collimation at injection in LHC. In green the circulating beam envelope. In red the deflected beam trajectory due to channeling in a 60  $\mu$ rad bent crystal. In red the Cherenkov radiator location. In orange the location of the secondary absorber.

FIG. 3. Simulation of the horizontal crystal-assisted collimation in collision in LHC. In green the circulating beam envelope. In red the deflected beam trajectory due to channeling in a 60  $\mu$ rad bent crystal. In red the Cherenkov radiator location. In orange the location of the secondary absorber.

FIG. 4. A particular view of the piezoelectric goniometer for LHC

FIG. 5. A particular view of the piezoelectric goniometer for LHC

FIG. 6. A particular view of the piezoelectric goniometer for LHC

FIG. 7. The setup for the HiRadMat test of a LHC crystal.

FIG. 8. The thin Cherenkov radiator installed close to the absorber of the SPS.

FIG. 9. The results of the Cherenkov radiator at the BTF in Frascati. In green the data relative to the upright position of the radiator with respect to the incoming beam. In orange the data relative to the 45° position of the radiator with respect to the incoming beam.

FIG. 10. The “hokey stick” radiator for the SPS in its vacuum tank.

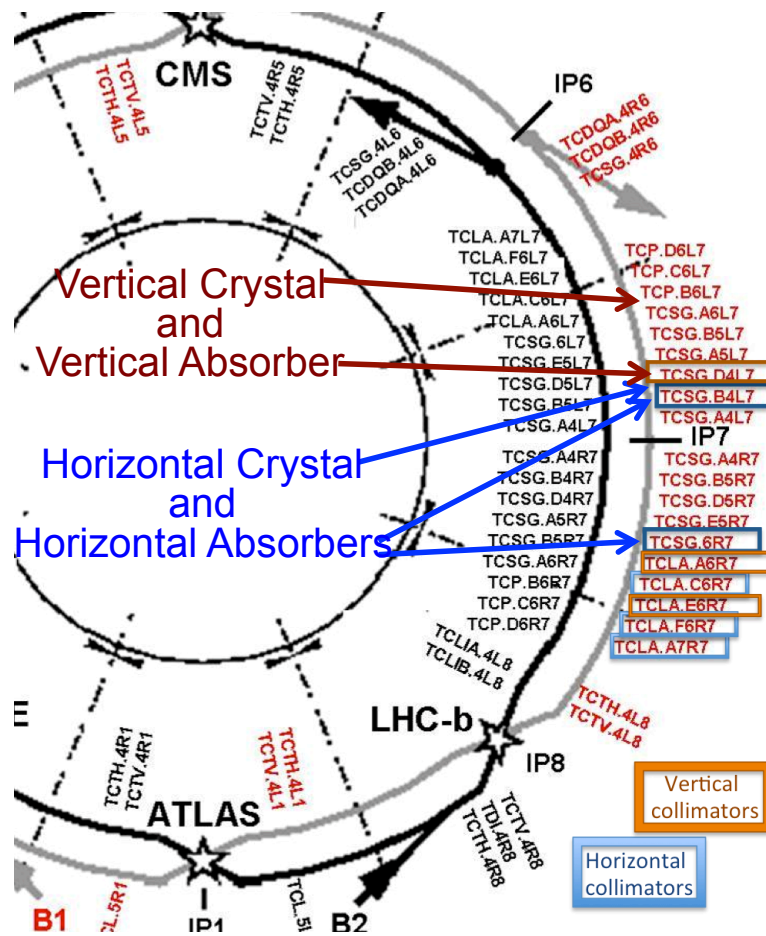


Figure 1

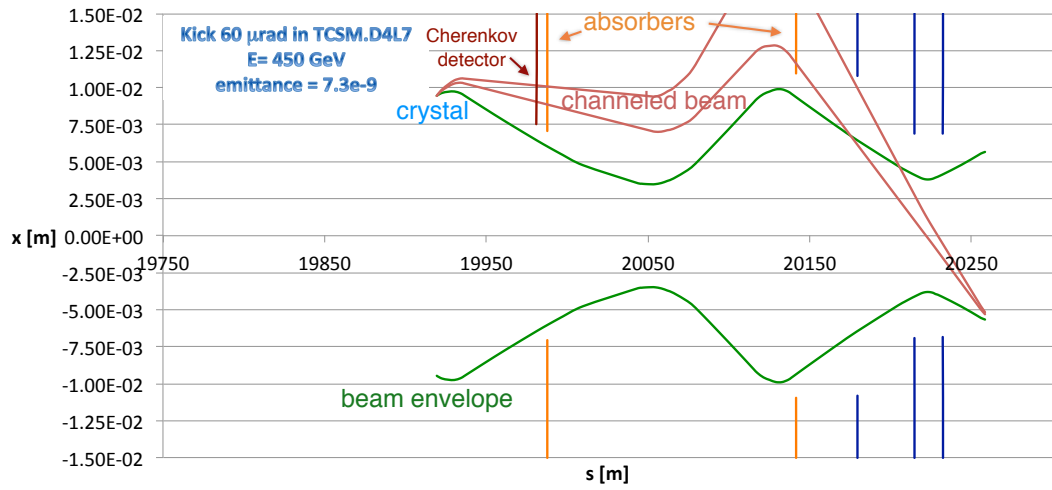


Figure 2

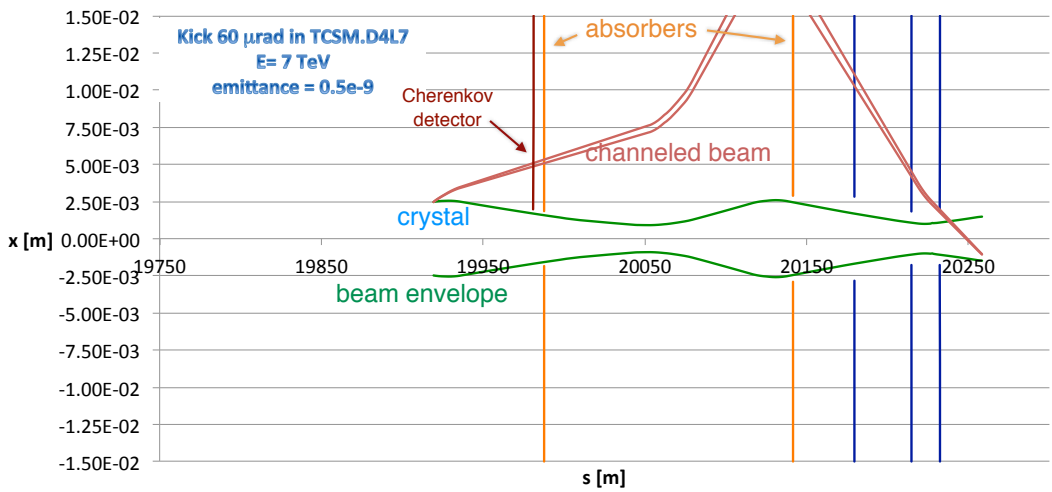
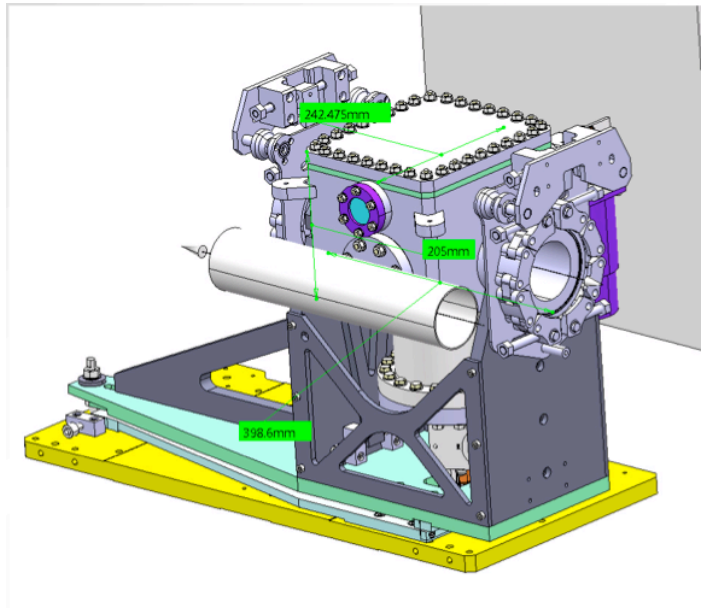
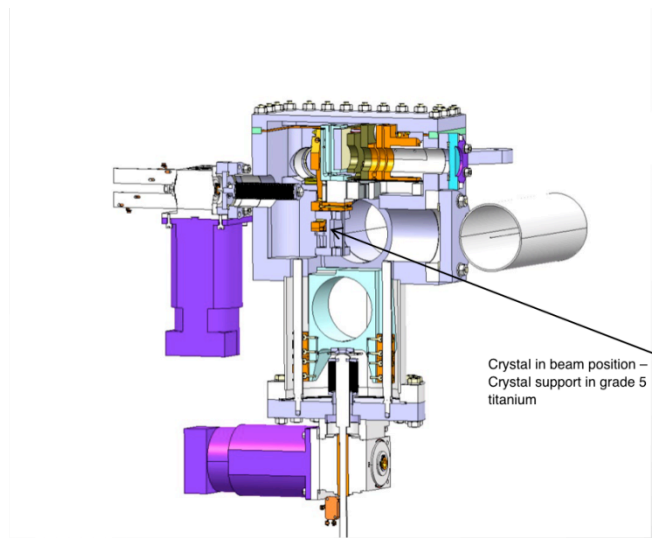


Figure 3



**Figure 4**



**Figure 5**

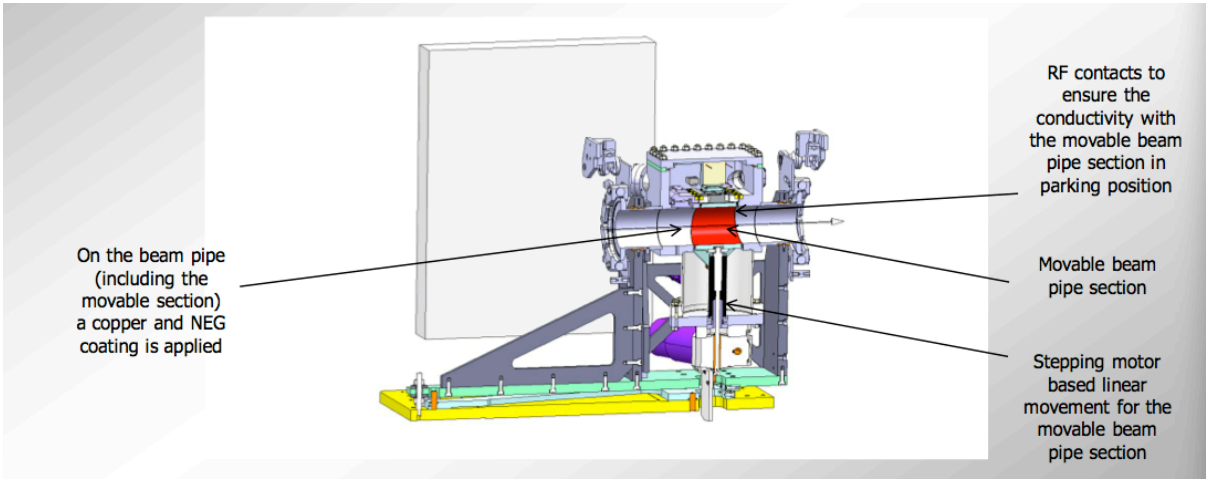


**Figure 6**



**Figure 7**

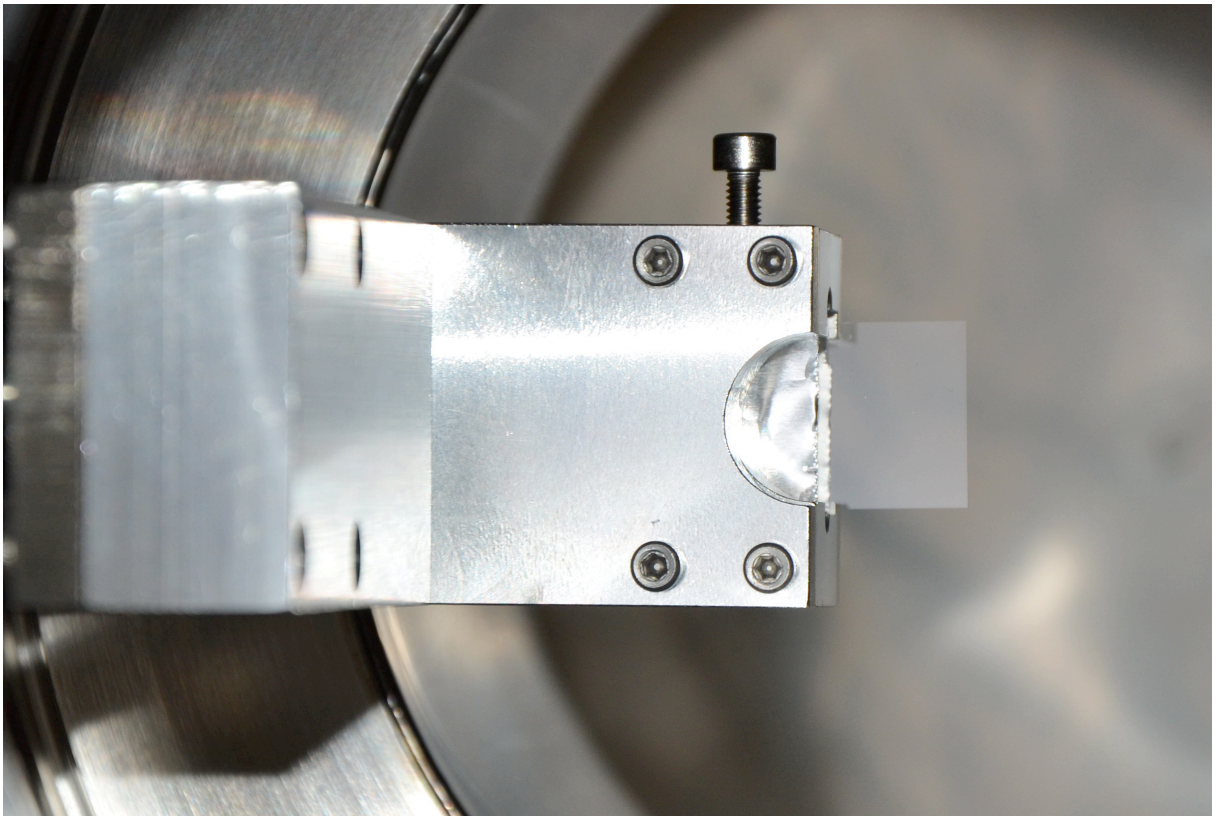


**Figure 8**

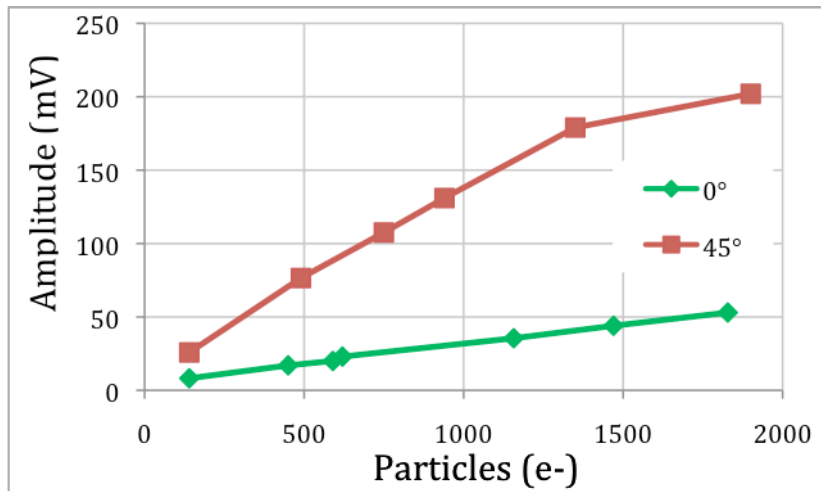


**Figure 9**

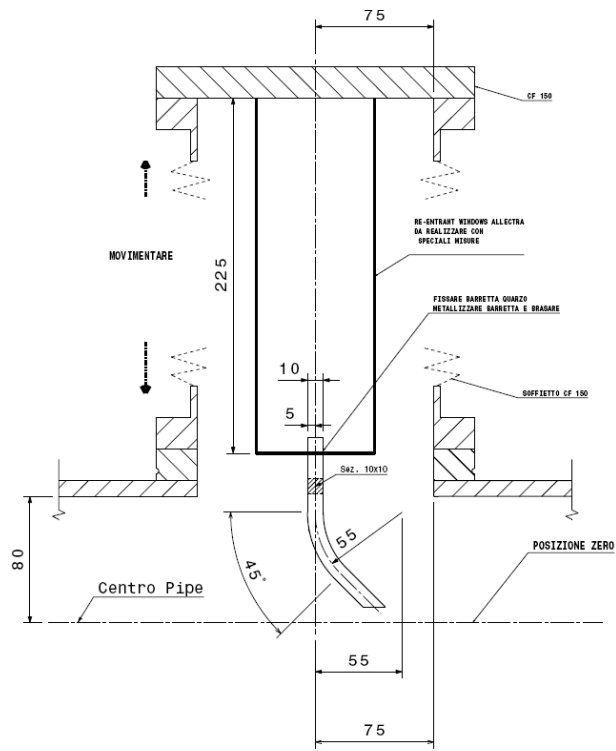


**Figure 10**